A&A manuscript no.
(will be inserted by hand later)

Your thesaurus codes are:
01(02.02.1; 02.01.2; 02.12.1; 11.09.1 MCG -6-30-15; 11.09.1 Mrk 766; 13.25.2)

ASTRONOMY AND ASTROPHYSICS
September 29, 2000

Soft X-ray emission lines from a relativistic accretion disk in MCG -6-30-15 and Mrk 766

G. Branduardi-Raymont[1], M. Sako[2], S. M. Kahn[2], A. C. Brinkman[3], J. S. Kaastra[3], and M. J. Page[1]

[1] Mullard Space Science Laboratory, University College London, Holmbury St. Mary, Dorking, Surrey, RH5 6NT, UK
[2] Department of Physics and Columbia Astrophysics Laboratory, Columbia University, 550 West 120th Street, New York, NY 10027, USA
[3] Space Research Organisation of the Netherlands, Sorbonnelaan 2, 3584 CA Utrecht, NL

Received 29 September 2000 / Accepted

Abstract. *XMM-Newton* Reflection Grating Spectrometer (RGS) spectra of the Narrow Line Seyfert 1 galaxies MCG -6-30-15 and Mrk 766 are physically and spectroscopically inconsistent with standard models comprising a power-law continuum absorbed by either cold or ionized matter. We propose that the remarkably similar features detected in both objects in the 5 – 35 Å band are H-like oxygen, nitrogen, and carbon emission lines, gravitationally redshifted and broadened by relativistic effects in the vicinity of a Kerr black hole. We discuss the implications of our interpretation, and demonstrate that the derived parameters can be physically self-consistent.

Key words: Black hole physics – Accretion, accretion disks – Line: formation – Galaxies: individual: MCG -6-30-15 – Galaxies: individual: Mrk 766 – X-rays: galaxies

1. Introduction

The precise shape of the low energy spectra of active galaxies has traditionally been very difficult to establish. The combined effects of interstellar absorption, moderate spectral resolution of available detectors, and intrinsic complexity in the sources have so far prevented us from determining even whether the underlying spectrum is mainly due to continuum emission, or includes discrete emission and absorption components. The model generally adopted to match the observations is that of a continuum spectrum absorbed by partially ionized material (Halpern 1984; Reynolds 1997, and references therein); the origin and location of this warm absorber at the core of active galaxies, however, is still very much matter of debate (e.g., Otani et al. 1996).

The enhancement in energy resolution and sensitivity afforded by the *XMM-Newton* Reflection Grating Spectrometer (RGS; den Herder et al. 2001) provides us with the potential to unravel the true origin of the soft X-ray emission in AGN for the first time. RGS observations of MCG -6-30-15 and Mrk 766, which are reported here, have forced us to examine alternatives to the warm absorber model, and to propose a new and radically different interpretation of the soft X-ray spectra of active galaxies.

Send offprint requests to: G. Branduardi-Raymont

2. MCG -6-30-15 and Mrk 766

MCG -6-30-15 and Mrk 766 (NGC 4253) are classified as Narrow Line Seyfert 1 (NLS1) galaxies on the basis of the widths of their Balmer lines (< 2000 km s^{-1}), although they are not of the extreme kind. Both show strong and rapid variability in their X-ray fluxes, as well as variability in the slope of their power-law continua. MCG -6-30-15 is not known to possess a "soft excess" (which is one of the dominant characteristics of this class of objects), while Mrk 766 displays a soft excess that varies less than the continuum at higher energies. Evidence for Compton reflection has been found only in MCG -6-30-15. Broad features in the < 1 keV spectra of both sources have been attributed to absorption in an ionized interstellar medium at some distance from the central massive black hole. The profile of the broad fluorescent Fe Kα line observed at 6 – 7 keV can be explained as due to the effects of relativistic motions and gravitational redshift in a disk surrounding the central black hole (Tanaka et al. 1995). MCG -6-30-15 and Mrk 766 are bright ($L_{2-10\mathrm{keV}} \sim$ few $\times\ 10^{43}$ erg s^{-1}) and nearby AGN (z = 0.00774 and 0.0129 for MCG -6-30-15 and Mrk 766, respectively), with relatively low Galactic absorption along the lines of sight (4.1×10^{20} cm^{-2} and 1.8×10^{20} cm^{-2}, respectively).

3. RGS observations and data analysis

MCG -6-30-15 was observed with *XMM-Newton* in July 2000 for a total of 120 ks; Mrk 766 in May 2000 for 55 ks. The RGS data were processed with the *XMM-Newton* Science Analysis Software. Source and background events were extracted by making spatial and order selections on the event files, and were calibrated by applying the most

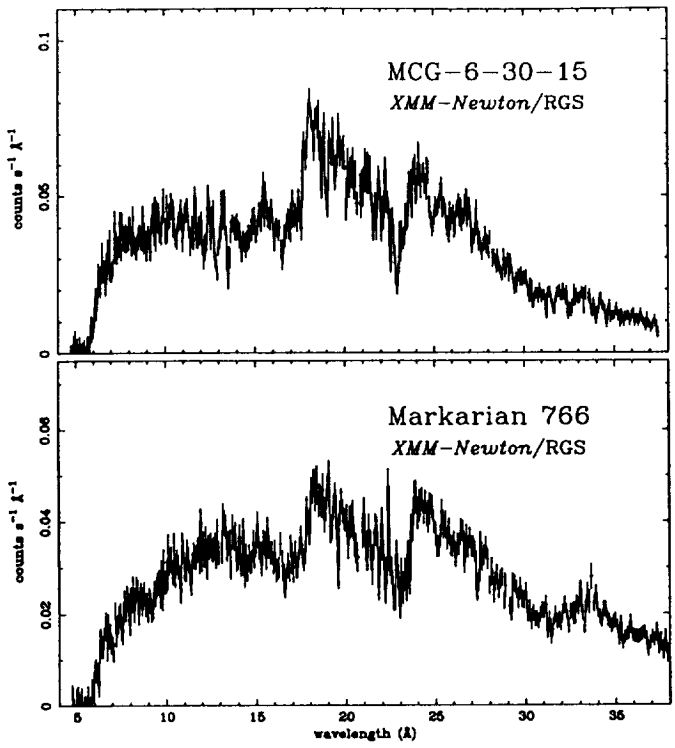

Fig. 1. The raw RGS first order spectra of MCG -6-30-15 (top) and Mrk 766 (bottom).

up-to-date calibration parameters. The current wavelength scale is accurate to ~ 8 mÅ, and the uncertainties in the effective area are $\leq 10\%$ in the 10 – 35 Å region and $\leq 20\%$ in the 5 – 10 Å. The instrumental oxygen edge was calibrated using observations of pure continuum sources, 3C 273, Mrk 421, and PKS 2155-304, as described in den Herder et al. (2001).

The raw extracted spectra are shown in Fig. 1. They are remarkably similar, in their overall shape and in the details, being dominated by prominent "saw-tooth" features, which peak at around 15, 18, 24 and 33 Å. A single power-law fit with neutral absorption is clearly an unacceptable representation of the observed spectra. In particular, the neutral oxygen edge at 23 Å implies too high a column density than can be accommodated by the fit to the continuum. In addition, the spectra do not show neutral absorption edges from the other elements at their expected positions.

3.1. Spectral Fits with Warm Absorber Models

We attempted to fit the spectra with a warm absorber model which includes the appropriate absorption edges and absorption lines associated with all ions of abundant elements (C, N, O, Ne, Mg, and Fe). The absorption line equivalent widths depend on the velocity profile, and we assume a turbulent velocity, which is a free parameter for each charge state. The absorbing column density of each charge state is also left free to vary. The fits (shown in Fig. 2) are unacceptable for both objects, for a number of reasons. Firstly, the observed, putative "O VIII and O VII edges" are redshifted with respect to their expected positions (14.23 Å and 16.78 Å for O VIII and O VII, respectively), and by very large amonts ($\sim$ 1 Å), corresponding to *infall* velocities on the order of $\sim 16,000$ km s^{-1}. Moreover, for the column densities derived from the putative edges, the absence of the associated absorption lines at the implied redshift for these two charge states implies an extremely small velocity width ($\Delta v \leq 60$km s^{-1}), which is difficult to reconcile with the apparent large velocity shift of the oxygen edges. The radial inflow, in this case, would have to be at one particular velocity. Re-emission following absorption is an unlikely explanation for the absence of the absorption lines. If the surrounding material is falling towards the nucleus, most of the material will be re-emitting radiation at shorter wavelengths than that of the absorbed resonance line, and we would expect to observe an inverted P Cygni profile, which is definitely not in the data.

The fits described above still require a significant neutral absorbing component in excess of the Galactic column density to these sources. In the case of Mrk 766, the neutral oxygen edge is again too high with respect to what is required to fit the data at longer wavelengths. An excess of flux is also present between 18 and 19 Å in MCG -6-30-15.

3.2. Disk-line Emission Interpretation

The physical and spectroscopic implausiblities described above force us to examine alternative models to reproduce the observed RGS spectra. Remarkably, we have been able to obtain acceptable fits to both the MCG -6-30-15 and Mrk 766 data with a completely different model consisting of an absorbed power-law and emission lines, which are gravitationally redshifted and broadened by relativistic effects in a medium which is circling around a massive, rotating black hole. In this interpretation, the saw-toothed features in Fig. 1 are attributed to (in ascending wavelength order) H-like O VIII Lyβ, O VIII Lyα, N VII Lyα and C VI Lyα line emission.

Our model includes a power-law continuum, with cold absorption fixed at the Galactic value, and four emission lines represented by profiles originating near a maximally rotating Kerr black hole (Laor 1991). The line wavelengths are fixed at their expected values in the observer's frame for the redshifts of the sources. The continuum power-law slope (photon index Γ) is fitted, as are the disk inclination angle i, the emissivity index q (i.e., the slope of the radial emissivity profile in the disk), and the inner and outer limits $R_{\rm in}$ and $R_{\rm out}$ of the disk emission region. These parameters are tied for all the lines in the fit.

The best fit parameters are listed in Table 1; data and best fit models are shown in Fig. 3 for both MCG -6-30-15 and Mrk 766. The errors quoted correspond to 90% confidence ranges for one interesting parameter. The derived

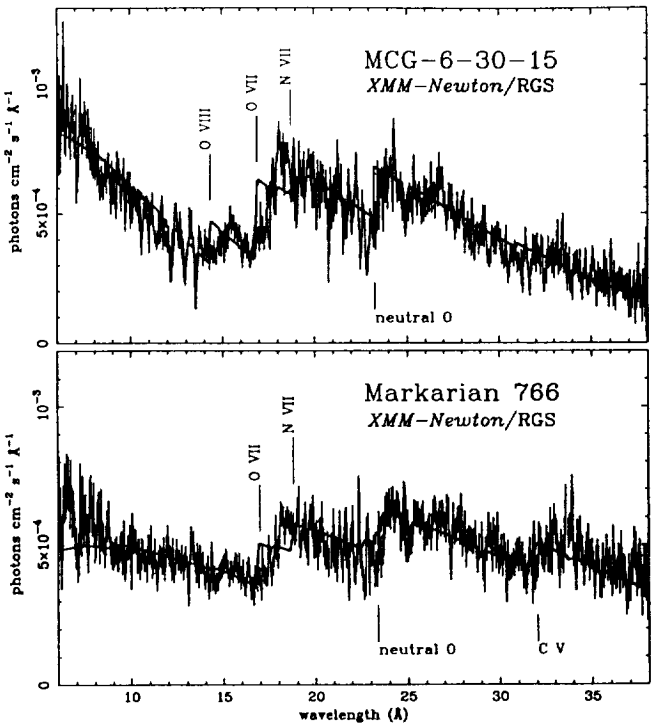

Fig. 2. "Fluxed" spectra of the two sources (corrected for effective area) with the best-fit warm-absorber model.

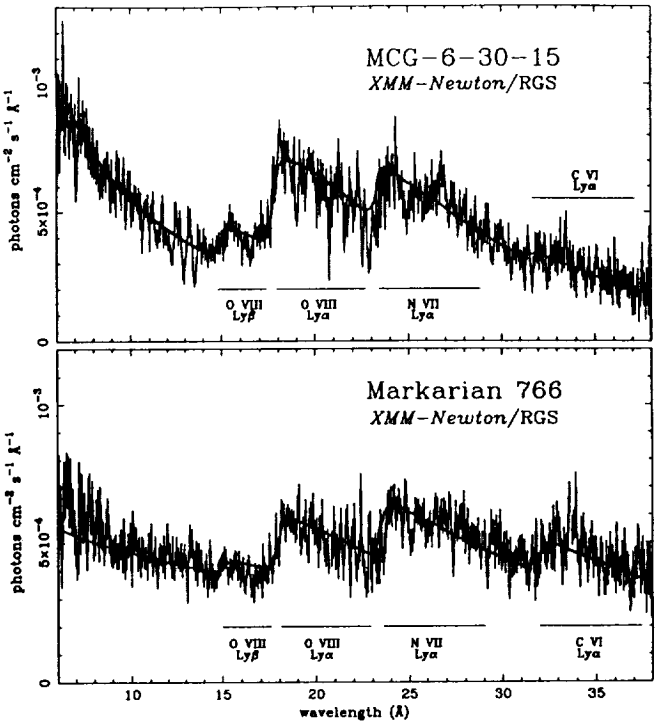

Fig. 3. Same as in Figure 2 with the relativistically broadened line model. The parameters are listed in Table 1

Table 1. Best fit parameters for isolated lines model

Parameter	MCG − 6 − 30 − 15	Mrk766
Γ	1.01 ± 0.01	1.63 ± 0.03
Inclination i	$36.8° \pm 0.3°$	$35.1° \pm 0.9°$
Emissivity index q	3.97 ± 0.05	3.59 ± 0.09
$R_{\rm in}$	$1.24^{+0.7}_{-0.0}$	$1.24^{+0.8}_{-0.0}$
$R_{\rm out}$	110^{+90}_{-60}	50^{+60}_{-15}
CVI Lyα[a]	$(8.2 \pm 1.3)\,10^{-4}$	$(1.2 \pm 0.1)\,10^{-3}$
NVII Lyα[a]	$(2.6 \pm 0.1)\,10^{-3}$	$(1.9 \pm 0.1)\,10^{-3}$
OVIII Lyα[a]	$(4.6 \pm 0.1)\,10^{-3}$	$(1.9 \pm 0.1)\,10^{-3}$
OVIII Lyβ[a]	$(1.4 \pm 0.1)\,10^{-3}$	$(4.0 \pm 0.4)\,10^{-4}$

[a] Observed line intensities in units of ph cm^{-2} s^{-1}

emissivity index of $q \sim 4$ indicates that most of the line emission originates from the inner part of the disk where gravitational effects are the strongest. The outer emission radius is, therefore, not well-constrained. For the same reason, disk emission line profiles produced in a Schwarzschild metric (Fabian et al. 1989) do not provide an acceptable fit to the data, since the last stable orbit, in this case, is substantially larger than that in the Kerr metric.

It is worth stressing again that both galaxies exhibit essentially an identical spectral structure, with multiple broadened lines of H-like oxygen, nitrogen and carbon. The line energies are consistent with the galaxies systemic velocities, and all lines are consistent with having the same broad profiles. The fit residuals are also much less obvious and systematic than for the warm absorber model. In addition, the disk line parameters are consistent with those derived for the Fe Kα line (Nandra et al. 1997). No additional column density to the Galactic value is required by the fits. All of these factors, which are consistent with each other to a degree that makes chance coincidences unlikely, imply that the relativistic line model is the most probable explanation for the present observations.

The models in Fig. 3 deliberately do not include absorption features, in order to emphasize the quality of the line emission fit. We have re-fitted the spectra including, in addition to the four emission lines, narrow absorption lines. No edges are required by the data. Lines from Ne IX and X, Fe XIX – XXI, O VII and O VIII Lyα, N VII and C VI Lyα are detected in MCG -6-30-15, while only oxygen, nitrogen, and carbon lines appear in Mrk 766. In contrast to the pure warm absorber fit, the absorption lines profiles are well-reproduced by the model with much lower ion column densities ($N_i \leq 10^{17}$ cm^{-2}) and a higher velocity width ($FWHM$ $v_{turb} \sim 2000$ km s^{-1}). The observed line positions in MCG -6-30-15 are slightly blueshifted from their rest wavelengths indicating outflow velocities of $v \sim 400$ km s^{-1}, while those in Mrk 766 are consistent with no net velocity shift. With such low column densities, no edges are expected to be detectable, as observed.

Table 2. Ion emission measures derived from self-consistent fits

Ion	MCG − 6 − 30 − 15	Mrk766
CVI Lyα[a]	$(0.65 \pm 0.13)\ T_{100\mathrm{eV}}^{0.65}$	$(3.6 \pm 0.4)\ T_{100\mathrm{eV}}^{0.65}$
NVII Lyα[a]	$(2.7 \pm 0.1)\ T_{100\mathrm{eV}}^{0.65}$	$(6.6 \pm 0.6)\ T_{100\mathrm{eV}}^{0.65}$
OVIII Lyα[a]	$(3.3 \pm 0.1)\ T_{100\mathrm{eV}}^{0.82}$	$(5.5 \pm 0.5)\ T_{100\mathrm{eV}}^{0.82}$

[a] Ion EMs in units of 10^{63} cm^{-3}.

4. Physical Consistency of the Relativistic Disk Emission Model?

The lack of Fe L and He-like K emission lines in the RGS spectra suggests that the observed emission lines are most likely due to radiative recombination onto fully stripped ions (oxygen is fully ionized for kT $\geq$ 100 eV; Kallman & Krolik 1995). We refit the spectrum self-consistently accounting for the higher Lyman series, as well as the radiative recombination continua (RRC), in a purely recombination-dominated plasma. We find that the fits are unacceptable if the RRC fluxes are fixed at their optically thin theoretical levels. As discussed below, however, there may be residual photoelectric opacity in the gas, which may partially suppress the RRC. Therefore, we allowed the normalizations of the RRC with respect to the lines to be free parameters in the fit. The best-fit model, which again includes the narrow absorption features, is shown in Figure 4. The derived ion emission measures ($EM_{i+1} = n_e n_{i+1} V$) for H-like carbon, nitrogen, and oxygen are listed in Table 2. As in the previous fit with the individual emission lines, the spectrum is well-reproduced by the model and the derived disk parameters are also very similar. For a maximally rotating black hole with $i \sim 37°$ and $q \sim 4$, most of the emitted flux is beamed away from the observer, and a correction factor is applied to the isotropic luminosity. Adopting the method of Cunningham (1975), we find $F_{\mathrm{obs}} \sim 0.3\ L_{\mathrm{em}}/4\pi D^2$, where F_{obs} is the observed fluxed, L_{em} is the emitted luminosity in the rest frame of the emitting material, and D is the distance to the source.

For a plasma in which the material is nearly fully stripped, the ratios of the ion EMs provide the abundance ratios directly. The observed ratios are $A_C/A_O = 0.28 \pm 0.05$ and $A_N/A_O = 0.76 \pm 0.05$ for MCG -6-30-15, and $A_C/A_O = 0.65 \pm 0.2$ and $A_N/A_O = 1.2 \pm 0.3$ for Mrk 766. These ratios are rather different (particularly for Mrk 766) from the solar values of $A_C/A_O = 0.43$ and $A_N/A_O = 0.13$ (Anders & Grevesse 1989). However, the strength of the nitrogen absorption lines in both MCG -6-30-15 and Mrk 766 suggests that nitrogen is overabundant in the extended absorbing medium as well. Such anomalies have also been inferred from UV observations of quasars (e.g., Hamann & Ferland 1992; Artymowicz, Lin, & Wampler 1993, and references therein).

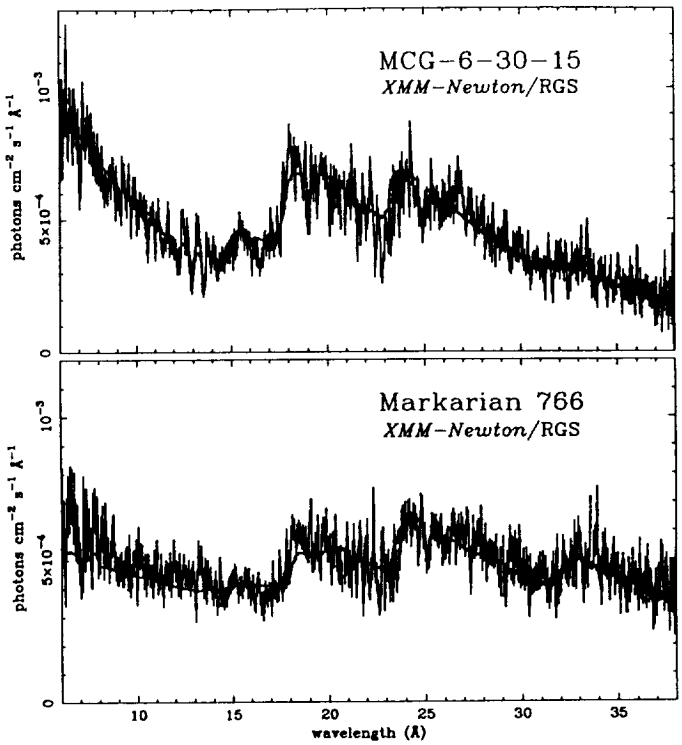

Fig. 4. Same as in Figure 2 with the self-consistent emission line model. The parameters are listed in Table 2

Using the derived parameters for MCG -6-30-15, we calculate the abundance-corrected total emission measure ($EM = n_e^2\ V$) for O VIII to be,

$$EM = 3.8 \times 10^{66}\ T_{100\mathrm{eV}}^{0.82}\ A_{\mathrm{O}\odot}^{-1}, \quad (1)$$

where $A_{\mathrm{O}\odot}$ is the oxygen abundance relative to the solar value.

Assuming a disk-like geometry, we estimate the total emission measure to be $EM \sim \pi n_e^2 R^2 H$, where R is the characteristic radius and H is the scale height of the emitting material. In the inner regions of a relativistic accretion disk where the pressure is dominated by radiation, the ratio of the scale height to the disk radius is on the order of $f = H/R \sim 10^{-3}$ (Kato, Fukue, & Mineshige 1998). Assuming that the characteristic emission radius is $R \sim 10\ R_g$, where $R_g = GM/c^2 = 1.5 \times 10^{12}\ M_7$ cm and M_7 is the mass of the black hole in multiples of $10^7 M_\odot$, we can estimate the average electron density to be,

$$n_e = 6.0 \times 10^{14}\ T_{100\mathrm{eV}}^{0.41}\ A_{\mathrm{O}\odot}^{-1/2}\ f_{-3}^{-1/2}\ M_7^{-3/2}\ \mathrm{cm}^{-3}, \quad (2)$$

where f_{-3} is the ratio H/R in multiples of 10^{-3}. The implied electron scattering optical depth in the vertical direction of the disk is,

$$\tau_e \sim n_e H \sigma_T = 6.0\ T_{100\mathrm{eV}}^{0.41}\ A_{\mathrm{O}\odot}^{-1/2}\ f_{-3}^{1/2}\ M_7^{-1/2}. \quad (3)$$

These simple estimates may be uncertain by as much as a factor of a few.

The moderate to high optical depth may present a potential problem. For $\tau_e \geq 5$, broadening of the spectral lines due to electron scattering becomes comparable to the broadening from gravitational and relativistic effects. If $\tau_e \leq 1$, however, electron scattering produces a negligible effect on the observed line profiles, and this situation is possible if, for example, the emission region is much smaller than the scale height of the accretion disk (i.e., $f_{-3} \ll 1$).

On the other hand, a medium in which $\tau_e \sim 1$ is required to explain the weaknesses of the RRC in our self-consistent fits. For both MCG -6-30-15 and Mrk 766, the fits require significantly reduced RRC for oxygen and somewhat reduced RRC for nitrogen and carbon. With trace abundances of the H-like species, however, the medium can be optically thick to its own RRC. In this case, recombination to the ground state is suppressed and most of the expected RRC flux is eventually radiated in Ly-series lines. It only takes an optical depth of order a few at the photoelectric edge in order achieve this. In O VIII, the threshold optical depth in the K edge is $\tau_{\rm OVIII} \sim 130\, \tau_e\, A_{\rm O\odot}\, f_{\rm OVIII}$, where $f_{\rm OVIII}$ is the fractional ion abundance of O VIII. Therefore, even a small trace abundance of O VIII can almost completely suppress the RRC. Since the Ne X and Ne IX emission line wavelengths are close to but shorter than that of the O VIII edge, most of these line photons are probably also absorbed by O VIII, which subsequently are pumped into the O VIII lines. The O VIII Lyα line wavelength is longer than that of the N VII edge, and is not affected by this opacity effect. However, the O VIII Ly-β and the higher series lines do lie above the N VII edge and should be somewhat affected. In addition, the N VII Ly-α line is just on the short wavelength side of the C VI edge. The effects of this opacity require detailed radiative transfer modeling, which is beyond the scope of this Letter.

To check for consistency in the parameters derived above, we compute the upper limit for the average ionization parameter of the plasma to be,

$$\xi = \frac{L}{n_e R^2} = 7 \times 10^3\, L_{43}\, T_{100\rm eV}^{-0.41}\, A_{\rm O\odot}^{1/2}\, f_{-3}^{1/2}\, M_7^{-1/2}, \quad (4)$$

which is consistent with the observed level of ionization in that C, N, and O should be nearly fully stripped. The temperature at this level of ionization is $kT \sim 200$ eV.

The same calculations have been applied to Mrk 766, with the following results:

$$EM = 6.3 \times 10^{66}\, T_{100\rm eV}^{0.82}\, A_{\rm O\odot}^{-1}, \quad (5)$$

$$n_e = 7.8 \times 10^{14}\, T_{100\rm eV}^{0.41}\, A_{\rm O\odot}^{-1/2}\, f_{-3}^{-1/2}\, M_7^{-3/2} {\rm cm}^{-3}, \quad (6)$$

$$\tau_e = 7.8\, T_{100\rm eV}^{0.41}\, A_{\rm O\odot}^{-1/2}\, f_{-3}^{1/2}\, M_7^{-1/2}. \quad (7)$$

The observed RGS spectra also require a flattening of the underlying continuum radiation in both MCG -6-30-15 and Mrk 766 below ~ 2.5 keV. A preliminary spectral analysis of the EPIC PN data of MCG -6-30-15 shows that a power-law slope of ~ 1 can reproduce the 1 - 2 keV spectrum, with substantial excess soft emission below ~ 1 keV. A simple extension of the 3 - 10 keV continuum down to lower energies also requires excess emission below ~ 1 keV. Most of the observed soft X-ray flux, however, is in the form of C, N, and O emission lines. If the hard X-ray continuum radiation is produced through inverse Compton scattering primarily of these line photons, the apparent break in the photon index may be a natural consequence (Sunyaev & Titarchuk 1980).

Clearly the results we present here and their interpretation in terms of line emission from a relativistic disk call for a complete re-assessment of the processes leading to the production of high energy radiation in the cores of active galaxies. Such a study will have to account for the flattening of the hard X-ray continuum towards low energies as well as the detailed line-formation processes in the inner regions of the accretion disk.

5. Conclusions

We have shown that a simple warm-absorber interpretation of the RGS spectra of MCG -6-30-15 and Mrk 766 is untenable, on both spectroscopic and physical grounds. Broad line emission from a relativistic disk surrounding a maximally rotating Kerr black hole seems to explain the data remarkably well. The physical self-consistency of this scenario remains to be established, however, the preliminary analysis presented in Sec. 4 is encouraging. Note that the conclusions we draw do not depend on any preconceived assumption on the shape of the ionizing continuum.

This result could not have been achieved without the combination of large effective area and high energy resolution afforded by the *XMM-Newton* RGS. The poorer resolution of CCD spectrometers cannot provide discriminatory power for the warm absorber versus line emission debate raised by the RGS results presented in this paper. A more robust test will be finding the same problems and applying the same solution to other AGN sources.

Acknowledgements. The Mullard Space Science Laboratory acknowledges financial support from the UK Particle Physics and Astronomy Research Council. The Columbia University team is supported by NASA. The Laboratory for Space Research Utrecht is supported financially by the Netherlands Organization for Scientific Research (NWO).

References

Anders, E., & Grevesse, N. 1989, Geochim. Cosmochim. Acta, 53, 197

Artymowicz, P., Lin, D. N. C., & Wampler, E. J. 1993, ApJ, 409, 592

Cunningham, C. T. 1975, ApJ, 202, 788

den Herder, J. W., et al. 2001, this volume

Fabian, A. C., Rees, M. J., Stella, L., & White, N. E. 1989, MNRAS, 238, 729
Halpern, J. P. 1984, ApJ, 281, 90
Hamann, F., & Ferland, G. 1992, ApJ, 391, L53
Kallman, T. R., & Krolik, J. H. 1995, XSTAR – A Spectral Analysis Tool, HEASARC (NASA/GSFC, Greenbelt)
Kato, S., Fukue, J., & Mineshige, S. 1998, Black-hole Accretion Disks (Kyoto: Kyoto University Press)
Laor, A. 1991, ApJ, 376, 90
Kallman, T. R. and Kahn, S., 1996, ApJ, 465, 994
Nandra, K., George, I. M., Mushotzky, R. F., Turner, T. J. & Yaqoob, T. 1997, ApJ, 477, 602
Otani, C., Kii, T., Reynolds, C. S., Fabian, A. C., Iwasawa, K., Hayashida, K., Inoue, H., Kunieda, H., Makino, F., Matsuoka, M. and Tanaka, Y. 1996, PASJ, 48, 211
Reynolds, C. S. 1997, MNRAS, 286, 513
Sunyaev, R. A., & Titarchuk, L. G. 1980, A&A, 86, 121
Tanaka, Y., et al. 1995, Nature, 375, 659